

- 43–49. In M.R. Carter (ed.) Soil sampling and methods of analysis. Lewis Publ., Boca Raton, FL.
- Turtola, E., and A. Jaakkola. 1995. Loss of phosphorus by surface runoff and leaching from a heavy clay soil under barley and grass ley in Finland. *Acta Agric. Scand.* 45:159–165.
- Vanasse, A., R.R. Simard, and G.D. Leroux. 1997. Qualité des eaux de drainage sous billons: essais à la ferme. [Drainage water quality under ridge tillage]. p. 73–81. In CPVQ. Colloque sur le semis direct et la culture sur billons. 12–13 février 1997. St-Hyacinthe, QC.
- Webster, R., and M.A. Oliver. 1990. Statistical methods in soil and land resource survey. Oxford Univ. Press, New York.
- Yuan, G., and L.M. Lavkulich. 1995. Environmental phosphorus indices in manure amended soils in the Fraser basin of British Columbia, Canada. *J. Environ. Sci. Health B30*, 6:841–857.
- Zhang, T.Q., A.F. MacKenzie, and B.C. Liang. 1995. Long-term changes in Mehlich-3 extractable P and K in a sandy clay loam soil under continuous corn (*Zea mays* L.). *Can. J. Soil Sci.* 75:361–367.

DIVISION S-5—PEDOLOGY

Preferential Flow and Pedotransfer Functions for Transport Properties in Sandy Kandiudults

J. N. Shaw,* L. T. West, D. E. Radcliffe, and D. D. Bosch

ABSTRACT

Soils with differences in argillic and kandic horizon clay content (12–28% clay), thickness of overlying sandy eluvial horizons (ranging from <0.50 to >1.0 m), and degree of structural development occur in upland Kandiudult soils in the Upper Coastal Plain of Georgia. Interest in agricultural site-specific management necessitates more adequate characterization of solute transport properties between and within these soils. Undisturbed columns (15-cm diam., $n = 34$) were collected by horizon for three pedons typifying the extremes of the clay content in the argillic horizon. Breakthrough curves (BTCs) were conducted using a Br^- tracer and were evaluated by fitting the single- and two-region adaption of the convection–dispersion equation (CDE) to outflow measurements. Saturated hydraulic conductivity (K_s) measurements and methylene blue dye staining of conducting voids were also performed on the cores. Dye staining indicated differences in preferential flow occurred between surface (Ap), eluvial (E), and argillic and kandic (Bt) horizons. Retardation factors (R) were positively correlated with clay quantities, and horizons possessing relatively less clay (A and E horizons) possessed the highest α values (quickest solute exchange rates between mobile and immobile regions). Horizons with relatively higher clay quantities (Bts) had the lowest α and β (ratio of mobile water to the volumetric water content) values, but the highest effective dispersivity (λ_{eff}) values. Dye-stained areas were correlated ($r = 0.65$) with β , which suggested β may be an approximation of the degree of preferential flow for these soils. For the three pedons studied, significant differences in α existed between the extremes, and thus they are interpreted to behave differently from a solute transport standpoint. Pedotransfer functions (PTFs) were developed for grossly estimating hydraulic and transport parameters.

BREAKTHROUGH CURVES have been used as both a qualitative and quantitative assessment of water and solute transport in soils (Gupte et al., 1996; Ghodrati, 1995; Veeh et al., 1994; Jury et al., 1991; Bouma, 1991; Brusseau and Rao, 1990). Often, BTCs are simultane-

ously optimized with solute transport equations (such as the single-domain CDE, or a dual-domain nonequilibrium mobile–immobile [MIM] adaption to the CDE) to estimate parameters with implied physical interpretation (Jensen et al., 1996; Jury et al., 1991; Yamaguchi et al., 1989; van Genuchten and Wierenga, 1976). Problems exist because model parameters generally are not independently measurable, although correlation has been found between parameters and certain soil properties (Vervoort et al., 1999; Shaw et al., 1997; Bajracharya and Barry, 1997; Rao et al., 1980b). Although these models have adequately characterized transport at the column scale, questions remain as to their applicability to large-scale heterogeneous transport phenomena (Jensen et al., 1996). More recently, researchers have started to develop methods of estimating model parameters independent of optimization techniques, allowing a greater predictive capacity and enhanced mechanistic validity of the models (Brusseau et al., 1994). Pedotransfer functions, or models which relate basic soil properties to more complex soil hydraulic functions, may be a method to independently assess model parameters (Wosten et al., 1995; Vereecken et al., 1990, 1992).

Investigators have shown the amount of biological activity and the degree of expression (grade) and shape of soil structure can have a large impact on solute transport paths and BTC results (Vervoort et al., 1999; Starett et al., 1996; Li and Ghodrati, 1994; Bouma, 1991). Soil structure develops from biological activity and the shrinking and swelling of aggregates due to alternating wetting and drying. Shrinking and swelling is more predominant in clayey or loamy soils than in coarser soils (Horn et al., 1995). Because of this, horizons with more clay typically have better expression of structure than sandier soils.

Where structure and biological activity have resulted in increased macropore influence on transport processes, two-domain nonequilibrium models simulating

J.N. Shaw, Auburn Univ., Dept. of Agronomy and Soils, 202 Funchess Hall, Auburn, AL 36849; L.T. West and D.E. Radcliffe, Univ. of GA., Dept. of Crop and Soils, 3111 Miller Plant Sci. Bldg., Athens, GA 30602; D.D. Bosch, USDA-SE Watershed Laboratory, P.O. Box 946, Tifton, GA, 31794. Received 13 Oct. 1998. *Corresponding author (jnshaw@acesag.auburn.edu).

Abbreviations: BTC, breakthrough curve; CDE, convection–dispersion equation; MIM, mobile–immobile; PTF, pedotransfer functions; PVC, polyvinyl chloride; TDR, time domain reflectometry.

preferential flow are assumed to have increased validity (Gerke and van Genuchten, 1993). Rao et al. (1980b) showed that more tailing or asymmetry in BTCs resulted from increased aggregate sizes, which is directly related to soil structure and macropore predominance. As described by Brusseau and Rao (1990), the mechanisms involved with the two-domain MIM adaption to the CDE include: (i) the convective and dispersive movement of solute in the bulk solution to the boundary of an adsorbed water layer, (ii) the diffusion across the boundary, and (iii) the intrapedal and intra-aggregate diffusion within the immobile regions. This intra-aggregate diffusion process (within micropores) is typically considered to be the rate-limiting step (Brusseau and Rao, 1990).

Soils with varying thicknesses of sandy epipedons overlying sandy to loamy argillic horizons occur in portions of the Upper Coastal Plain of Georgia. These soils have typically been mapped as Typic, Arenic, and Grossarenic subgroups of Kandudults, indicating eluvial sand thicknesses of <0.50 to >1 m overlying argillic horizons. These soils are sometimes mapped in the same associations. Within map units, these soils possess differences in the amount of clay in the argillic horizon, the predominant structure in the solum, and thicknesses of overlying sandy mantles. It is hypothesized that this varying degree of argillic horizon expression and differences in structure and sandy eluvial horizon thickness manifest in varying degrees of preferential flow in these soils, resulting in contrasting transport characteristics. Because these soils are extensive in this region and are commonly used for peanut (*Arachis hypogaea* L.) and cotton (*Gossypium hirsutum* L.) production, differences in hydraulic and transport properties might necessitate more detailed (larger-scale) mapping for precision-farming applications. Interpedon structural attributes

vary as well, with sandy eluvial horizons possessing essentially no structure (described as single grain), and loamier subsurface horizons possessing weak or moderate grades of subangular blocky structure. Evaluation of these interpedon attributes (by horizon) are necessary because many simulation models require inputs by horizon, and soil survey data are collected in such a manner. The objectives of this study were (i) to examine the effects of sandy epipedons and contrasting argillic horizon expression on transport properties within pedons, (ii) to determine if differences in solute transport properties occur within this map unit, and (iii) to develop possible PTFs to estimate some of these hydraulic and transport parameters.

MATERIALS AND METHODS

The research site, near Plains (Sumter County), GA (Fig. 1) ($31^{\circ}59'0''$ to $45''$ N, $84^{\circ}24'0''$ to $30''$ W), was located in the southern portion of the Fall Line Hills region. In this region, soils have developed from Eocene-aged fluvio-marine sediments. Along the crest of a hillslope on a narrow interfluvium at this site, a reconnaissance soil survey was conducted (25 observations), and three sampling sites were chosen to be typical of the contrasting soils observed on these landscapes (J.N. Shaw, 1999, unpublished data). Sampling pits will be referred to as the NW, NE, and SE pedons (Fig. 1). Bulk samples were collected by horizon per standard soil survey technique (Soil Survey Staff, 1996).

Soils in this study possessed different thicknesses of sandy eluvial horizons (E) over highly weathered red subsoils of relatively low pH, which consisted mainly of quartz, kaolinite, gibbsite, and Fe oxides (J.N. Shaw, 1999, unpublished data). The highly weathered mineralogical suites translated to subsoils possessing low activity, and the pedons classified into subgroups of Kandudults (Table 1). Analyses of proximate pedons not included in this study also displayed the kandic nature of the subsoils for these pedons (J.N. Shaw, 1999, un-

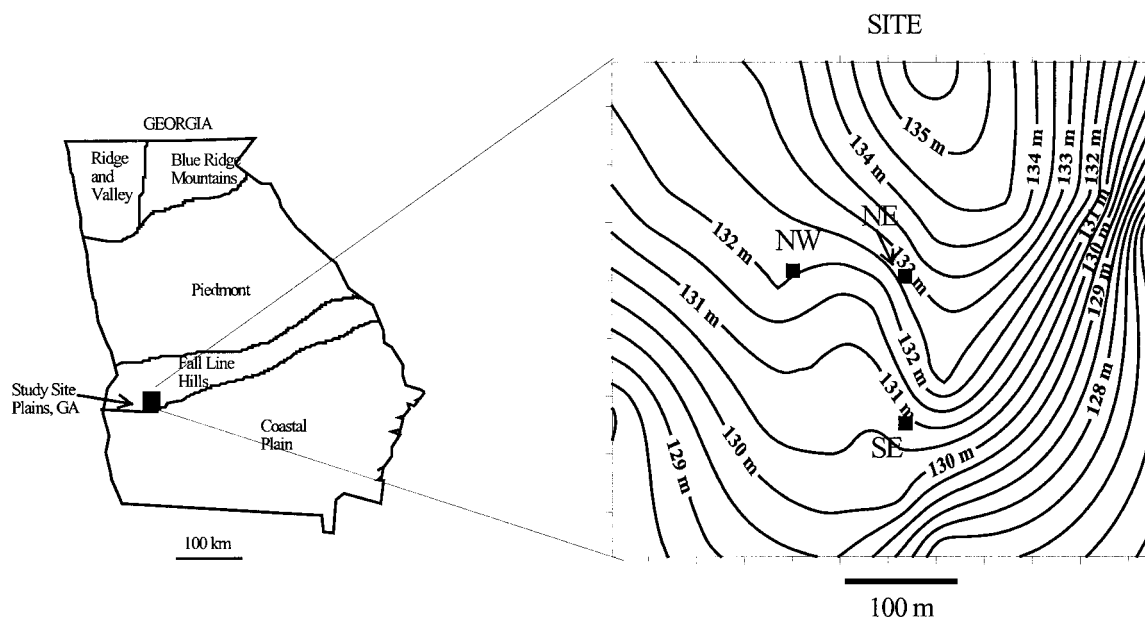


Fig. 1. Location of study site near Plains, GA, with subset of sampling locations. Contour intervals (0.5 m) are shown.

Table 1. Physical and chemical properties for three pedons.†

Horizon	Depth cm	Color	Structure‡	Sand Silt Clay			CEC cmol _c kg ⁻¹	ECEC	ρ _b Mg m ⁻³
				%					
NW (loamy, kaolinitic, thermic Grossarenic Kandiudult)									
Ap	0–12	7.5YR 4/4	1 f gr	90.6	6.0	3.4	1.86	1.08	1.77
A/E	12–26	7.5YR 4/4	0 sg	90.8	6.8	2.5	1.44	0.41	1.72
E1	26–75	2.5YR 4/8	0 sg	89.7	6.3	4.1	0.89	0.26	1.70
E2	75–109	2.5YR 4/8	0 sg	89.2	6.4	4.4	0.85	0.69	1.62
E3	109–138	2.5YR 4/8	0 sg	88.3	6.0	5.8	0.89	0.68	1.65
Bt1	138–191	2.5YR 4/8	1 m sbk	81.0	3.8	15.2	2.15	1.13	1.70
Bt2	191–240	2.5YR 4/8	1 m sbk	82.8	3.2	14.1	1.11	0.94	–
BC	240–300	2.5YR 4/8	1 m sbk	87.9	2.5	9.7	0.81	0.38	–
SE (coarse-loamy, kaolinitic, thermic Typic Kandiudult)									
Ap	0–21	7.5YR 4/6	1 f gr/pl	84.9	12.5	2.7	2.27	0.79	1.71
Bt1	21–52	2.5YR 4/6	1 f&m sbk	77.1	11.4	11.6	2.01	0.81	1.67
Bt2	52–92	2.5YR 4/6	1 f&m sbk	75.9	10.9	13.2	2.15	0.89	1.61
Bt3	92–126	10R 4/6	2 m sbk	75.3	8.5	16.3	2.51	1.34	1.65
Bt4	126–164	10R 4/6	2 m sbk	66.1	5.9	28.1	3.11	1.89	1.69
Bt5	164–250	10R 4/6	2 m sbk	68.0	5.0	27.1	2.65	1.04	1.73
NE (loamy, kaolinitic, thermic Grossarenic Kandiudult)									
Ap	0–26	10YR 3/3	1 f gr/pl	89.1	7.2	3.7	1.96	1.10	1.69
E	26–110	5YR 4/6	0 sg	83.3	7.7	9.0	1.65	0.46	1.63
Bt	110–250	2.5YR 4/6	2 m sbk	75.8	3.2	21.0	1.98	1.30	1.71

† CEC is cation-exchange capacity; ECEC is effective cation-exchange capacity; ρ_b is bulk density.

‡ 0 = structureless, 1 = weak, 2 = moderate, 3 = strong; f = fine, m = medium; gr = granular, sbk = subangular blocky, pl = platy.

published data). Surface (A) and eluvial horizons (E) were coarse-textured (sand and loamy sand), while Bt horizons ranged from loamy sand to sandy clay loam in texture (Table 1). In most situations, surface horizons (Ap) had weak granular structure, E horizons were structureless (single grain), while Bt horizons possessed weak to moderate grades of subangular blocky structure (Table 1). The sites had been fallow for several years before the soils were sampled.

Undisturbed cores ($n = 37$, 15-cm diam., average length = 19.9 ± 4.1 cm, range = 11.0–29.2 cm) were extracted from the SE, NE, and NW pedons by excavating to the horizon of interest and carving a column of soil that could be encased by 15-cm-diameter polyvinyl chloride (PVC) pipe. Encased cores were separated at the base, trimmed, and packed for transport to the laboratory. The PVC casing was carefully removed from the columns, and each was coated with liquid saran and a 5- to 10-mm layer of paraffin to seal column sides against wall flow. Because of the morphological similarities, NW surface horizons (Ap and A/E), eluvial horizons (E1, E2, and E3) and SE Bt1 and Bt2 horizons were sampled separately but grouped for comparisons. For comparison of certain results, horizons were grouped into three classes based on tex-

ture and structural attributes (Table 1), that is, sandy (SE Ap; NW Ap, E1, E2 and E3, and BC; NE Ap and E), loamy (SE Bt1 and Bt2, SE Bt3), and clayey (SE Bt4, SE Bt5, and NE Bt). Class names do not coincide with U.S. soil taxonomy definitions. Saturated hydraulic conductivities on these cores were measured with the constant head method (Klute and Dirksen, 1986). After steady flow was established with a 0.025 M KNO₃ solution, BTCs were measured using a 2 g L⁻¹ Br⁻ tracer. Bromide was added as a pulse input (1/10 of a pore volume), and leachate samples were collected sequentially until three to four pore volumes of Br⁻ solution had been collected. Bromide leachates were analyzed with an ion-specific electrode using a double junction reference electrode in a 0.05 M NaNO₃ solution to adjust ionic strength. Volumetric water content was measured in the columns by time domain reflectometry (TDR) (10-cm rod) after BTC measurements and before blue dye staining.

Solute transport parameters were estimated by evaluating BTCs with CXTFIT (Parker and van Genuchten, 1984) using the single-region CDE (mode 2 of CXTFIT) and the two-region nonequilibrium MIM adaption of the CDE (mode 4). The two-region model is written as:

Table 2. Measures values (V, R, and dyed area) and estimated parameters using CXTFIT (Parker and van Genuchten, 1984) averaged for each horizon for the single-region and dual-region nonequilibrium model.†

Site	Horizon	R	t	n	V	V _M	D _{CDE}	D _{MIM}	λ _{CDE}	λ _{MIM}	θ _m /θ(β)	α	Dyed area‡	K _s
NW	Ap, A/E	1.41	s	2	1.92	2.41	2.54	1.42	1.34	0.56	0.79	3.41	100.0a	19.1
NW	E1, E2, E3	1.33	s	5	1.98	2.12	2.47	2.61	2.45	2.38	0.93	58.11	100.0a	25.7
NW	Bt1	1.75	l	2	0.78	2.33	6.43	5.11	7.66	1.58	0.39	1.91	67.5bc	19.1
NW	Bt2	1.46	l	2	1.02	2.37	8.14	8.27	7.11	4.61	0.52	3.30	76.4ab	25.8
NW	BC	1.51	s	2	2.00	2.71	7.80	7.43	3.91	2.84	0.74	31.74	96.5a	51.4
SE	Ap	1.20	s	2	0.89	1.14	1.70	1.73	1.85	1.49	0.79	4.66	97.0a	9.7
SE	Bt1, Bt2	1.16	l	3	1.24	1.33	3.58	5.05	4.07	4.57	0.88	8.69	93.0ab	25.3
SE	Bt3	1.41	l	3	1.50	1.83	2.37	2.30	2.78	2.42	0.85	12.51	100.0a	17.3
SE	Bt4	2.22	c	3	0.16	0.26	1.10	0.80	7.10	3.51	0.61	0.14	47.3c	2.3
SE	Bt5	2.25	c	3	0.19	0.70	0.48	0.18	2.38	0.30	0.26	0.11	18.9d	2.3
NE	Ap	1.13	s	2	1.30	1.33	0.72	0.75	0.56	0.55	0.95	26.93	100.0a	16.9
NE	E	1.37	s	2	2.43	3.38	2.49	2.78	0.88	0.81	0.83	40.30	93.6ab	30.3
NE	Bt	1.75	c	3	0.19	48.93	0.19	0.12	0.97	0.32	0.36	0.20	65.8c	2.4

† R = retardation factor (measured), t = textural grouping, where s = sandy, l = loamy, c = clayey; V = pore water velocity and V_M = V/β, β = θ_m/θ, D_{CDE} and D_{MIM} = dispersion coefficients for the two models, λ_{CDE} and λ_{MIM} = dispersivity for the two models, and α is the exchange coefficient.

‡ Same letter indicates not significantly different (P = 0.05).

Table 3. Measured and model-derived average values for the three types of horizons separated by textural attributes.

Horizon type	n	Measured			MIM†				
		Blue dyed‡	R‡	V	D _{MIM} ‡	λ _{MIM} ‡	λ _{eff} §	α‡	θ _m /θ‡ (β)
		%	cm min ⁻¹	cm ² min ⁻¹	cm		min ⁻¹		
Sandy	15	98.7a (88.0–100)¶	1.31b (1.13–1.51)	1.83 (0.68–3.10)	2.75b (0.28–12.74)	1.63a (0.12–4.92)	2.1b (0.34–9.58)	33.6a (0.02–142.15)	0.86a (0.70–1.00)
Loamy	10	89.2a (52.8–100)	1.42b (1.16–1.75)	1.16 (0.42–2.31)	4.88a (0.28–12.78)	3.34a (0.22–6.35)	6.0ab (0.36–32.34)	7.4b (0.01–34.41)	0.70a (0.27–0.93)
Clayey	9	44.0b (16.8–100)	2.07a (1.75–2.25)	0.18 (0.10–0.27)	0.37c (0.04–1.61)	1.38a (0.01–6.99)	331.0a (2351.43–2.50)	0.2b (0.00–0.37)	0.41b (0.00–0.66)

† MIM = mobile-immobile model output.
 ‡ Same letter indicates not significantly different (P = 0.05).
 § Same letter indicates not significantly different (P = 0.10).
 ¶ Range for values.

$$\theta_m R \left(\frac{\partial C_m}{\partial t} \right) + \theta_{im} R \left(\frac{\partial C_{im}}{\partial t} \right) = \theta D_m \left(\frac{\partial^2 C_m}{\partial z^2} \right) - \theta V_m \left(\frac{\partial C_m}{\partial z} \right) \quad [1]$$

$$\theta_{im} R \left(\frac{\partial C_{im}}{\partial t} \right) = \alpha (C_m - C_{im}) \quad [2]$$

where *t* is time (min), *z* is depth (cm), θ_m is volumetric water content in the mobile fraction; θ_{im} is volumetric water content in the immobile fraction, θ = θ_m + θ_{im}, C_m is the concentration of solute in mobile fraction (mg L⁻¹), C_{im} is the concentration of solute in immobile fraction (mg L⁻¹), D_m is the dispersion coefficient (cm² m⁻¹), V_m is the pore water velocity (cm min⁻¹), R is the retardation factor (unitless), and α is the first-order rate constant (min⁻¹).

CXTFIT applies a nonlinear, least squares inversion method to evaluate transport parameters (Parker and van Genuchten, 1984). Prior to analyses of undisturbed cores, retardation factors (*R*) were measured using packed (bulk density = 1.50 g cm⁻³) columns (5 cm diam. by 20 cm long) of soil, a Br⁻ pulse input (2 g L⁻¹) at a constant pore water velocity (*V*), and the single-region CDE (Mode 2). Packed cores were used to evaluate *R* values to minimize physical flow effects on *R* values resulting from two-domain flow. By maintaining a constant *V* (*J_w*/θ, where *J_w* = *Q*/*A*, and *Q* is outflow [cm³ min⁻¹] and *A* is the cross-sectional area of flow [cm²]) and using packed cores, we assumed that the single-region CDE applied. The single-region model was then fit to the undisturbed cores keeping *V* (measured) and *R* (from packed cores) fixed. In this manner, *D*_{CDE} and λ_{CDE} (*D*_{CDE}/*V*) were estimated and calculated, respectively.

The two-region MIM model was used to estimate *D*_{MIM}, β (≈θ_m/θ), and α for all horizons (keeping *R* and *V* fixed), and λ_{MIM} [(*D*_{MIM}β)/*V*] and *V*_m(*V*/β) were calculated from these parameters. The α coefficient estimated the first-order rate of exchange between the mobile and immobile regions. The β parameter was interpreted to be equivalent to the ratio of mobile water to the volumetric water content (θ_m/θ) (using an

assumption made by Nkedi-Kizza et al., 1984). The β parameter is generally considered not to vary under different flow regimes (Bajracharya and Barry, 1997), although there has been evidence to the contrary (Brusseu et al., 1994). The model fits of all columns were evaluated, and modeling results were satisfactorily obtained on 34 of 37 columns.

Each column was leached with the cationic methylene blue dye after BTCs were completed (Shaw et al., 1997; Gupte et al., 1996). The dye was leached through the column until complete breakthrough was achieved as analyzed by a spectrophotometer. The cores were allowed to dry, and horizontal cuts (minimum of two) were made through each column to evaluate the dye-stained area using an image analysis technique. Cuts were made below the depth of insertion of the TDR rods (> 10 cm); however, in the four shortest columns, this was not possible. These columns were completely dyed (100%) and occurred in horizons where other cores were completely dyed, thus we believe these columns were minimally affected by dye movement along TDR rod holes. A video camera equipped with a frame grabber and image analysis software was used to collect the data. Camera magnification and screen resolution in the image analysis technique resulted in a pixel equivalent diameter area of ≈0.05 mm. Individual dye-stained areas <2 pixels were deleted, which resulted in analysis of dye-stained areas with equivalent diameter of >0.10 mm. Cross-sectional areas (percentage) of dye staining were then measured using the software, and percentages of dyed areas were averaged for the cuts within a column. The variability of the cross-sectional area of dye staining at different locations (cuts) within the individual cores was minimal for horizons that were essentially completely dye stained, with the average standard deviation being 9.3% for horizons that were not completely dyed. The depth distribution of dye staining within the columns (i.e., within a horizon) was not investigated.

Physical and chemical properties of the soils are given in Table 1. Particle-size determination was conducted on all hori-

Table 4. Pearson correlation coefficients (r) between soil properties and hydraulic and transport properties and parameters (n = 34).

Soil Properties†	V	V _M	R	D _{MIM}	λ _{MIM}	λ _{eff}	θ _m /θ(β)	α	K _s
Sand percentage	0.66***	-0.26	-0.75***	0.23	-0.07	-0.29	0.53**	0.47**	0.60***
Clay percentage	-0.68***	0.31	0.87***	-0.18	0.02	0.32	-0.66***	-0.45**	-0.59***
CEC	-0.60***	0.15	0.56***	-0.39*	-0.06	0.20	-0.36*	-0.54**	-0.62***
ECEC	-0.63***	0.07	0.58***	-0.35*	0.01	0.05	-0.33	-0.45**	-0.70***
Fe _d	-0.69***	0.31	0.90***	-0.12	0.03	0.35*	-0.70***	-0.43*	-0.55***
Fe _e	-0.56***	0.34	0.73***	-0.22	-0.21	0.24	-0.71***	-0.30	-0.53***
Cross-sectional dyed area	0.67***	-0.40*	-0.85***	0.27	0.04	-0.42*	0.65***	0.36*	0.62***
Size of structure‡	-0.64***	0.19	0.54***	0.07	0.06	0.18	-0.57***	-0.47**	-0.44**

*, **, *** Correlation coefficients significant at the 0.05, 0.01, and 0.001 levels, respectively.
 † CEC is cation-exchange capacity; ECEC is effective cation-exchange capacity; Fe_d is dithionite-citrate-bicarbonate extractable Fe on a Fe₂O₃ basis; Fe_e is oxalate extractable Fe on a Fe₂O₃ basis.
 ‡ Size of structure refers to structure size which is dependent on the type of structure. Adjusting for these differences, median values for each class were used as input. For structureless horizons, median particle size was used.

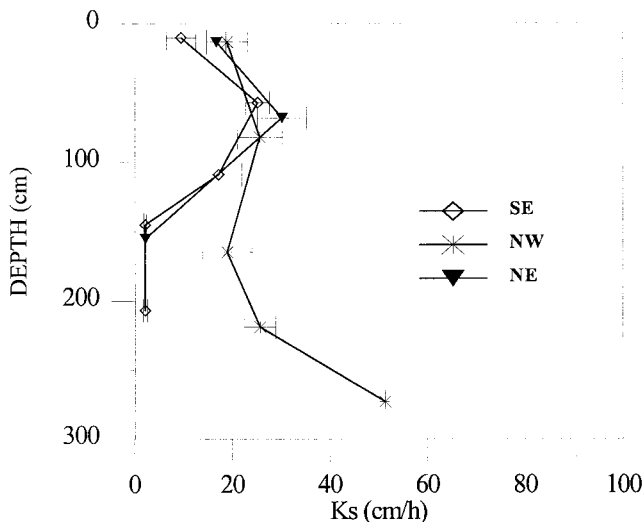


Fig. 2. Saturated hydraulic conductivity, K_s , with depth for the three pedons. Bars represent standard errors of means.

zons by the pipette method (Kilmer and Alexander, 1949). Basic cations (Ca, Mg, K, and Na) were extracted with 1 M NH_4OAC (pH 7) using an autoextractor (Soil Survey Investigations Staff, 1996) and were measured using atomic absorption spectroscopy. Aluminum was extracted with 1 M KCl and was measured by atomic absorption spectroscopy (Soil Survey Investigations Staff, 1996). Effective cation-exchange capacity was computed by summing extractable cations and KCl-extractable Al. Cation-exchange capacity was obtained by the 1 M NH_4OAC (pH 7) method (Soil Survey Investigations Staff, 1996). Poorly crystalline Fe oxides and organically bound Fe were extracted with acid ammonium oxalate, and total Fe oxides were extracted with citrate-bicarbonate-dithionite (Jackson et al., 1986).

RESULTS AND DISCUSSION

Saturated Hydraulic Conductivity and Pore Water Velocities

Sandy horizons had the highest ($P = 0.05$) pore water velocities (V) (1.83 cm min^{-1}) followed by loamy horizons (1.16 cm min^{-1}) and clay enriched horizons (0.18 cm min^{-1}) (Tables 2 and 3). Therefore, V was inversely correlated with clay content ($r = -0.68$) (Table 4). Saturated hydraulic conductivity (K_s) decreased in the horizons possessing the highest clay content for all pedons (Fig. 2), and thus K_s was correlated with particle size (sand, $r = 0.60$; clay, $r = -0.59$) (Table 4). The lower K_s of the surface horizons (A) vs. the E horizons in the NW and NE and the upper Bt horizons of the SE was hypothesized to be due to the presence of a traffic pan near the base of the A horizons.

Dye Staining

Blue dye-stained cross-sectional areas tended to decrease with depth, except in the NW pedon, where the cross-sectional dyed area increased in the deeper BC horizons (Table 2, Fig. 3). Thus, proceeding downward and into the argillic horizon of all pedons, the area of blue dye staining decreased. Comparing the different horizon types between pedons (grouped as sandy,

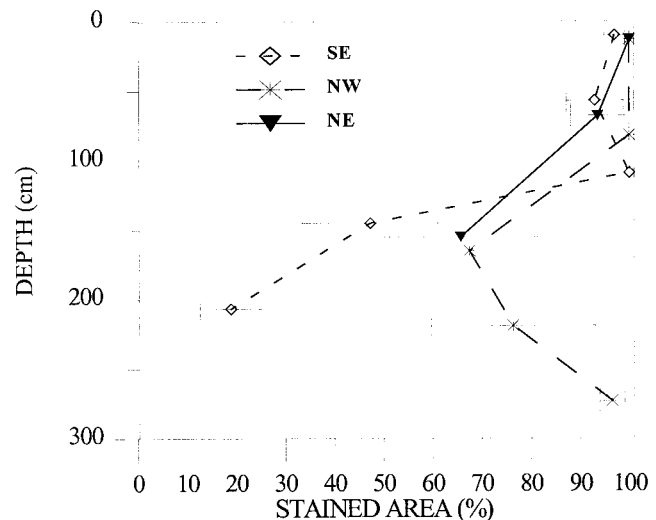


Fig. 3. Cross-sectional area of blue dye staining with depth. Bars represent standard errors of the means.

loamy, and clayey horizon types as discussed in the methods) showed significant differences ($P = 0.05$) in dye-stained area between sandy (98.7% dyed) and loamy horizons (89.2% dyed) as compared with horizons with more clay (44.0% dyed) (Table 3). Overall, dye-stained area amounts were negatively correlated with clay content ($r = -0.78$). Dye patterns for horizons exhibiting some degree of preferential flow are shown in Fig. 4. Figures 4a to 4c display a gradual decrease in dyed areas in Bt horizons from the NW (4a) to the NE (4b) to the SE (4c) pedons. These horizons exhibited stronger grades of structure than eluvial horizons (Table 1). Within pedons, a larger proportion of matrix type flow occurred in sandy and loamy horizon types than in horizons enriched with clay.

Retardation Factors

Retardation factors (R) for packed columns were found to be significantly ($P = 0.05$) lower in sandy (1.31) and loamy (1.42) horizons than horizons enriched with clay (2.07) (Table 3) and were correlated ($r = 0.87$) with clay content (Table 4). In these highly weathered, slightly acid systems, some anion-exchange capacity associated with kaolinite, gibbsite, or Fe oxides probably exists, and thus it is not surprising to see R for an anionic tracer correlated with clay content for these soils (Bellini et al., 1996).

A single-domain model (conventional CDE) was initially hypothesized to more adequately describe solute transport in the sandy epipedons, whereas a two-domain nonequilibrium model (MIM) was hypothesized to be more applicable in the underlying argillic horizons. Alternatively, Saxena et al. (1994) found that a dual porosity model more adequately predicted solute breakthrough than the conventional CDE in both unstructured sandy and structured clayey soils. Analyses of representative BTCs for horizons from these pedons illustrate differences in the BTC types observed (Fig. 5). As exhibited by the NE E horizon, many of the sandy horizon BTCs exhibited tailing of the effluent

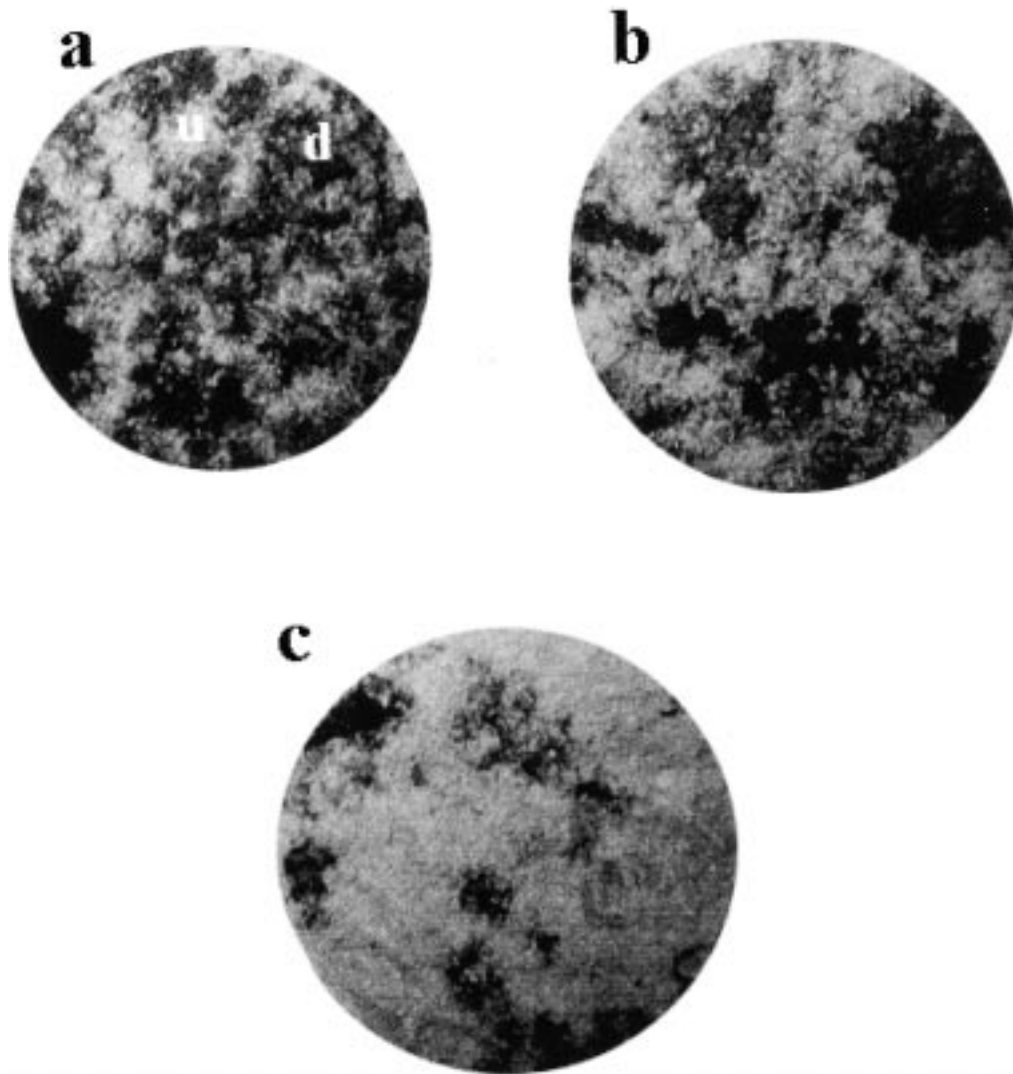


Fig. 4. Patterns of methylene blue dye staining from three cores (15-cm diam) showing undyed (u) and dyed (d) areas. (a) NW Bt1 horizon, (b) NE Bt horizon, (c) SE Bt4 horizon.

breakthrough similar to the Bt horizons shown, lending evidence that some degree of nonequilibrium flow occurred in sandy horizons (Fig. 5). Thus, the shape of the BTCs suggested a two-domain (region) modeling was more valid than a single-region model throughout these profiles. For this reason, we will concentrate on MIM modeling output below.

Breakthrough Curve Parameters

β Coefficient

Within all three pedons, β (assumed to be $= \theta_m/\theta$) coefficients tended to decrease with depth (Fig. 6). The β coefficient was correlated with clay content ($r = -0.66$) (Table 4). Significant correlation was found between β and percentage of blue dye-stained cross-sectional area ($r = 0.65$) (Table 4). We interpreted this to suggest β is an indication of the amount of cross-sectional area contributing to flow in these soils.

Sandy and loamy horizons had similar ($P = 0.05$) estimates of β (0.86 and 0.70, respectively). Horizons

with higher clay had lower β estimates (0.41), indicating a lower proportion of θ_m (Table 3). These data concurred with blue dye-stained area data that showed increased preferential flow was occurring in argillic horizons of all pedons.

α Coefficient

The α coefficient estimated the first-order rate of exchange between the mobile and immobile regions and has been shown to be related to V and the mean ped size (Kookana et al., 1993; Nkedi-Kizza et al., 1984; Rao et al., 1980a, 1980b). Bajracharya and Barry (1997) found that α was linearly related to V in each of three packed artificial cores where V was increased for each trial. Interestingly, although V was not adjusted within columns to test this dependency, when all cores were evaluated together, α was correlated with V ($r = 0.53$). Alpha values did not display any correlation with depth (Fig. 7), although sandy horizons were shown to have a significantly ($P = 0.05$) quicker α (33.6 min^{-1}) than both loamy (7.4 min^{-1}) and clayey (0.2 min^{-1}) horizons

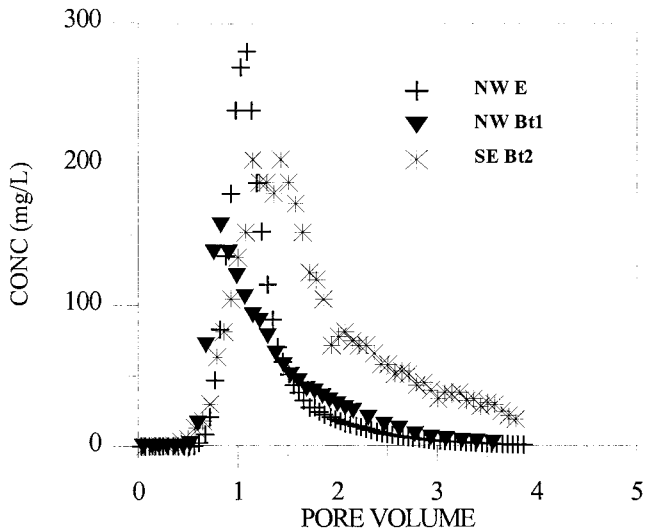


Fig. 5. Example of breakthrough curves from three horizons.

(Table 3). Similarly, α was found to be correlated with sand content ($r = 0.47$) (Table 4). Thus, relatively quicker rates of solute exchange occurred between mobile and immobile regions in sandy horizons. Some authors have indicated that a lower α implies increased ped size (Vervoort, 1999; Rao et al., 1980b), which might occur in some Bt horizons. We hypothesize that in these soils, lower α values may be due to increased grades of structure. This hypothesis is based on two observations. First, horizons possessing the lowest α values exhibited the most developed structure in the profile. Second, when α values from sandy horizons were evaluated for A, E, and BC horizons, A horizons had significantly ($P = 0.10$) lower α values than E horizons (11.7 vs. 53.0 min^{-1} , respectively), with BC horizons lying intermediate (31.7 min^{-1}). A horizons possessed weak grades of granular structure, while E horizons were structureless.

In order to examine size and α relationships more closely, a numerical scale was developed to describe

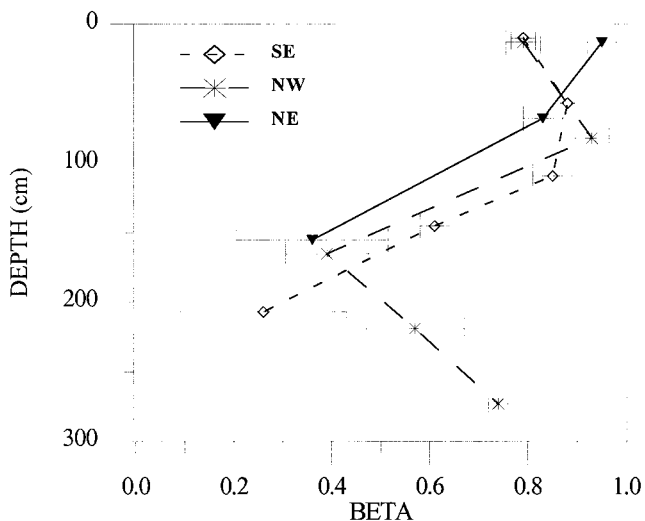


Fig. 6. Beta (ratio of mobile water to the volumetric water content) from the dual-domain nonequilibrium mobile-immobile (MIM) adaption to the CDE with depth for all pedons. Bars represent standard errors of means.

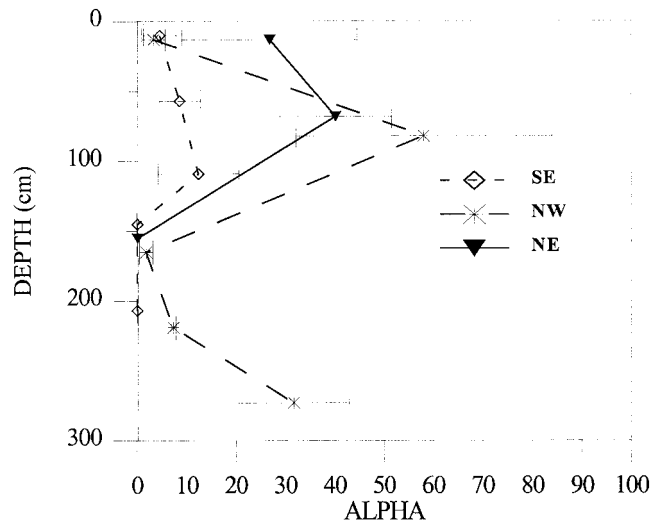


Fig. 7. Alpha from the dual-domain nonequilibrium mobile-immobile (MIM) adaption to the convection-dispersion equation with depth for all pedons. Bars represent standard errors of means.

structure size. The input values for structure characteristics were based on soil description (Table 1) data. A structure size numerical scale was established in which median values of the size ranges for the type of structure exhibited were used. The median value for the same descriptor (e.g., fine, medium) is different for different structures. For example, the size limits of fine classes for granular and subangular blocky structure are different, 1 to 2 and 5 to 10 mm for granular and subangular blocky, respectively; thus 1.5 or 7.5 mm would be chosen for these classes, respectively. Structureless horizons (sandy E horizons) were given a value of 0.4 mm, representing the mean particle size for these sandy horizons. Horizons exhibiting two structure sizes were given average values between both classes. Using this approach, α values were found to be correlated with size of structure ($r = -0.47$) (Table 4). This is in concurrence with other above-mentioned studies.

Dispersivity

Dispersivity (λ) values at the column scale have been shown to be correlated with pore-size distributions and size and grade of soil structure. Higher λ indicates a more heterogeneous pore system or longer flowpath lengths. Some authors have found that increased λ values within columns are due to discontinuous macropores (Buttle and Leigh, 1997). Overall, low λ_{MIM} values were observed in these soils. At least for sandy horizons, this may be due to particle-size effects, and the poorly developed structure in many of the sandy horizons (Ta-

Table 5. Weighted averages of parameters (to 250 cm) for the three pedon types.†

Pedon	n	λ_{MIM}		α	$\theta_{n0} (\beta)$	Dyed	R
		cm	min^{-1}				
SE	2	2.61a	209.5a	5.19a	0.60a	63.24a	1.73a
NE	3	0.58a	73.2a	16.47ab	0.61a	75.52a	1.56a
NW	2	2.36a	5.8a	27.60bc	0.72a	88.34a	1.46a

† Same letter indicates not significantly different ($P = 0.05$).

Table 6. Pedotransfer functions (PTFs).

PTF	Coefficient of determination (r^2)
$K_s = 25.89 - (0.032)(\% \text{ clay}^2)$	0.44***
$R = 1.23 + (0.001)(\% \text{ clay}^2)$	0.86***
$D_{\text{MIM}} = 2.07 + (0.643)(\text{size}^{1/2}) - (0.009)(\% \text{ clay}^2)$	0.30**
$\beta = 1.096 - (0.020)(\% \text{ clay})$	0.43***
$\ln(\alpha) = 4.51 - (0.065)(\% \text{ clay}^2) - (0.010)(\text{cecg}^\ddagger)$	0.57***

*, **, *** Significant at the 0.05, 0.01, and 0.001 levels, respectively.

† Size refers to structure size.

‡ cecg = cation-exchange capacity per gram of clay.

ble 3). No differences ($P = 0.05$) in λ_{MIM} values between the three horizon types were found in our study.

An effective dispersivity (λ_{eff}) can be calculated to evaluate differences in BTCs. This value incorporates all parameters that are indications of nonequilibrium flow in the MIM and is calculated as follows (Vervoot et al., 1999; Vallochi, 1985):

$$\lambda_{\text{eff}} = \lambda_{\text{MIM}}\beta + \frac{V_m(1 - \beta)^2}{\alpha} \quad [3]$$

λ_{eff} was higher ($P = 0.10$) in clayey than sandy horizons (331.0 and 2.0 cm, respectively) and indicated there was less equilibrium flow in the clayey horizons. Blue dye staining and estimates of β indicated clayey horizons exhibited an increased degree of preferential flow. We interpret the high value for λ_{eff} in the clayey horizons as giving the same indication.

Comparison of Pedons

To evaluate differences in solute transport parameters among the three pedons, weighted averages of the BTC parameters for each profile were taken to a depth of 250 cm. Although this approach neglects the connectivity of flow paths, many simulation models that accept input by horizon also suffer from this limitation. It is suggested that this approach can allow for relative comparison between pedons.

Increased bypass flow would be expected to occur in the pedons with more clayey Bt horizons. This expectation was supported by overall lower quantities of blue dye staining and θ_m/θ values in the NE and SE pedons than in the NW pedon, although values were not significantly different (Table 5). Alpha was significantly higher in the NW (27.60 min^{-1}) than the SE (5.19 min^{-1}) pedon ($P = 0.05$), with the NE pedon lying intermediate (16.47 min^{-1}). The SE pedons had higher λ_{eff} than NW pedons (209.5–5.8 cm), although this was not significant. Thus, only significant differences in α existed between the sandy and the clayey pedons, with the loamy NE pedon being intermediate of the other two. We believe that from an interpretive standpoint, differences in α manifest in differing solute transport for pedons, thus the NW and SE soils are dissimilar. Thus, to develop improved management schemes, the development of an Order 1 soil survey at a larger scale would allow the separation of these units on the landscape, which would be beneficial because of these differences with regard to solute transport.

Pedotransfer Functions

Using correlation relationships (some are shown in Table 4), PTFs were developed to quantify relationships between more easily measured properties and hydraulic and transport parameters. These PTFs were developed for K_s , R , D_{MIM} , α , and β values (Table 6). Past studies have shown certain soil properties are correlated with hydraulic parameters (Wosten et al., 1995; Vereecken et al., 1990; McKeague et al., 1982). These data suggest similar relationships can be developed to acquire gross approximations of transport parameters and hydraulic properties in some soils, although it is quite evident that the measured soil properties do not account for all the variability observed in the hydraulic and transport parameters ($r^2 = 0.30$ – 0.86). These PTFs show the types of relationships that can be had; further evaluations are necessary to refine the relationships. Thus, keeping in mind the variability associated with the associated parameters, we feel general and gross relationships between soils with regard to solute transport can be assessed with certain soil survey data. The *National Soil Survey Handbook* (Soil Survey Staff, 1996) describes a method for estimating soil permeability using a combination of particle-size distribution, consistence, pore geometry, ped surface features, and structure. More research on these types of simple relationships may allow the use of soil survey data to approximate transport parameters as well.

CONCLUSIONS

In this study, we compared measured values (K_s , V , R , cross-sectional area of blue dye staining) and model estimated parameters (α , β , λ) between horizons and pedons. It was evident that increased preferential flow occurred with increased clay content and higher developed structure as compared with sandier horizons with less developed structure for all pedons. Our results also indicated sandier pedons had a faster exchange of solutes between mobile and immobile regions. We suggest that these data indicate the soils on these landscapes had differing solute transport characteristics, which would indicate it is important to separate these particular soil units during soil survey in the region.

Correlations between model parameters and physical soil properties were found, and PTFs were developed to estimate these model parameters. Although it was quite evident that soil properties could not account for all of the variability in the transport and hydraulic variables, it does appear that PTFs may be a valuable tool for gross approximation of hydraulic and transport properties in some soils. Further investigations need to develop relationships to grossly approximate these transport parameters for a wide variety of soils, allowing for expanded interpretation of soil survey data.

REFERENCES

- Bajracharya, K., and D.A. Barry. 1997. Nonequilibrium solute transport parameters and their physical significance; numerical and experimental results. *J. Contam. Hydrol.* 24:185–204.
- Bellini, G., M.E. Sumner, D.E. Radcliffe, and N.P. Qafoku. 1996.

- Anion adsorption through columns of highly weathered acid soil: Adsorption and retardation. *Soil Sci. Soc. Am. J.* 60:132-137.
- Bouma, J. 1991. Influence of soil macroporosity on environmental quality. *Adv. Agron.* 46:1-35.
- Brusseau, M.L., Z. Gerstl, D. Augustijn, and P.S.C. Rao. 1994. Simulating transport in an aggregated soil with the dual-porosity model: Measured and optimized parameter values. *J. Hydrol.* 163:187-193.
- Brusseau, M.L., and P.C. Rao. 1990. Modeling solute transport in structured soils: A review. *Geoderma.* 46:169-192.
- Buttle, J.M., and D.G. Leigh. 1997. The influence of artificial macropores on water and solute transport in laboratory soil columns. *J. Hydrol.* 191:290-314.
- Gerke, H.H., and M.Th. van Genuchten. 1993. A dual-porosity model for simulating the preferential movement of water and solutes in structured porous media. *Water Resour. Res.* 29:305-319.
- Ghodrati, L.Y. 1995. Transport of nitrates in soils as affected by earthworm activities. *J. Environ. Qual.* 24:432-438.
- Gupte, S.M., D.E. Radcliffe, D.H. Franklin, L.T. West, E.W. Tollner, and P.F. Hendrix. 1996. Anion transport in a Piedmont Ultisol. II. Local-scale parameters. *Soil Sci. Soc. Am. J.* 60:762-770.
- Horn, R., T. Baumgartl, R. Kayser, and S. Baasch. 1995. Effect of aggregate strength and stress distribution in structured soils. p. 31-52. *In* K.H. Hartge and B.A. Stewart. (ed.) *Soil structure: Its development and function.* Advances in Soil Science. CRC Press, Boca Raton, FL.
- Jackson, K.H., C.H. Lim, and L.W. Zelazny. 1986. Oxides, hydroxides, and aluminosilicates. p. 113-119. *In* A. Klute (ed.) *Methods of soil analysis.* Part 1. 2nd ed. Agron. Monogr. 9. ASA and SSSA, Madison, WI.
- Jensen, K.H., G. Destouni, M. Sassner. 1996. Advection-dispersion analysis of solute transport in undisturbed soil monoliths. *Soil Sci. Soc. Am. J.* 34:1090-1097.
- Jury, W.A., W.R. Gardner, and W.H. Gardner. 1991. *Soil physics.* John Wiley and Sons, New York.
- Kilmer, V.J., and L.T. Alexander. 1949. Methods of making mechanical analysis of soils. *Soil Sci.* 68:15-24.
- Klute, A., and C. Dirksen. 1986. Hydraulic conductivity and diffusivity: Laboratory methods. p. 687-734. *In* A. Klute (ed.) *Methods of soil analysis.* Part 1. 2nd ed. Agron. Monogr. 9. ASA and SSSA, Madison, WI.
- Kookana, R.S., R.D. Schuller, and L.G. Aylmore. 1993. Simulation of simazine transport through soil columns using time-dependent sorption data measured under flow conditions. *J. Contam. Hydrol.* 14:93-115.
- Li, Y., and M. Ghodrati. 1994. Preferential transport of nitrate through soil columns containing root channels. *Soil Sci. Soc. Am. J.* 58: 653-659.
- McKeague, J.A., C. Wang, and G.C. Topp. 1982. Estimating saturated hydraulic conductivity from soil morphology. *Soil Sci. Soc. Am. J.* 46:1239-1244.
- Nkedi-Kizza, P., J.W. Biggar, H.W. Selim, M.Th. van Genuchten, P.J. Wierenga, J.M. Davidson, and D.R. Nielsen. 1984. On the equivalence of two conceptual models for describing ion exchange during transport through an aggregated Oxisol. *Water Resour. Res.* 20:1123-1130.
- Parker, J.C., and M. Th. van Genuchten. 1984. Determining transport parameters from laboratory and field tracer experiments. *Virginia Agric. Exp. Stn. Bull.* 84-3.
- Rao, P.S.C., R.E. Jessup, D.E. Rolston, J.M. Davidson and D.P. Kilcrease. 1980a. Experimental and mathematical description of non-adsorbed solute transfer by diffusion in spherical aggregates. *Soil Sci. Soc. Am. J.* 44:684-688.
- Rao, P.S.C., D.E. Rolston, R.E. Jessup, and J.M. Davidson. 1980b. Solute transport in aggregated porous media: Theoretical and experimental observation. *Soil Sci. Soc. Am. J.* 44:1139-1146.
- Saxena, R.K., N.J. Jarvis, and L. Bergstrom. 1994. Interpreting non-steady state tracer breakthrough experiments in sand and clay soils using a dual-porosity model. *J. Hydrol.* 162:279-298.
- Shaw, J.N., L.T. West, C.C. Truman, and D.R. Radcliffe. 1997. Morphologic and hydraulic properties of soils with water restrictive horizons in the Georgia Coastal Plain. *Soil Sci.* 162:875-885.
- Soil Survey Investigation Staff. 1996. *Soil survey laboratory methods manual.* Soil Surv. Invest. Rep. 42. USDA-SCS, Natl. Soil Survey Center, Lincoln, NE.
- Soil Survey Staff. 1996. *National soil survey handbook.* USDA-NRCS, National Soil Survey Center, Lincoln, NE.
- Starett, S.K., N.E. Christians, T.A. Austin. 1996. Comparing dispersivities and soil chloride concentrations of turfgrass-covered undisturbed and disturbed soil columns. *J. Hydrol.* 180:21-29.
- Vallochi, A. 1985. Validity of the local equilibrium assumption for modeling sorbing solute transport through homogeneous soils. *Water Resour. Res.* 21:808-820.
- van Genuchten, M.Th., and P.J. Wierenga. 1976. Mass transfer studies in sorbing porous media: Analytical solutions. *Soil Sci. Soc. Am. J.* 40:473-479.
- Veeh, R.H., W.P. Inskeep, F.L. Roe, and A.H. Ferguson. 1994. Transport of chlorsulfuron through soil columns. *J. Environ. Qual.* 23: 542-549.
- Vereecken, H., J. Diels, J. Van Orshoven, J. Feyen, and J. Bouma. 1992. Functional evaluation of pedotransfer functions for the estimation of soil hydraulic properties. *Soil Sci. Soc. Am. J.* 56: 1371-1378.
- Vereecken, H., J. Maes, and J. Feyen. 1990. Estimating unsaturated hydraulic conductivity from easily measured soil properties. *Soil Sci.* 149:1-12.
- Vervoort, R.W., D.E. Radcliffe, and L.T. West. 1999. Soil structure development and preferential solute flow. *Water Resour. Res.* 35:913-928.
- Wosten, J.H.M., P.A. Finkeand, and M.J.W. Jansen. 1995. Comparison of class and continuous pedotransfer functions to generate soil hydraulic characteristics. *Geoderma* 66:227-237.
- Yamaguchi, T., P. Moldrup, and S. Yokosi. 1989. Using breakthrough curves for parameter estimation in the convection-dispersion model of solute transport. *Soil Sci. Soc. Am. J.* 53:1635-1641.